THE ANALYST
FULL PAPER
www.rsc.org/analyst

Gold and silver nanoparticles: A class of chromophores with colors tunable in the range from 400 to 750 nm

Yugang Sun and Younan Xia*

Department of Chemistry, University of Washington, Seattle, Washington 98195-1700, USA

Received 18th December 2002, Accepted 18th March 2003
First published as an Advance Article on the web 4th April 2003

This paper presents several solution-phase methods for the large-scale synthesis of metal nanoparticles with controllable compositions (*e.g.*, spherical nanoparticles of gold/silver alloys), morphologies (*e.g.*, nanospheres, triangular nanoplates, circular nanodisks, and nanocubes of silver), and structures (*e.g.*, solid *vs.* hollow colloids). Spectral measurements indicated that the positions of surface plasmon resonance (SPR) bands for these nanoparticles could be tuned by varying all these parameters. The number of SPR peaks was found to increase as the symmetry of the nanoparticles decreased. In addition to their use as chromophores with strong extinction coefficients, these nanoparticles could serve as a platform to probe binding events of chemical and biochemical species on their surfaces. Gold nanoshells with hollow interiors were, in particular, shown to exhibit a much higher sensitivity to environmental changes than gold solid colloids with roughly the same size.

Introduction

Nanoparticles made of silver and gold have been the focus of research for many decades as a result of their intriguing optical properties.[1] When dispersed in liquid media, these nanoparticles usually display very intense colors due to surface plasmon resonance (SPR), a feature that can be attributed to the collective oscillation of conduction electrons as induced by an electromagnetic field.[2] The SPR frequency of nanosized metal particles is different from that of bulk material and has been shown to strongly depend on their size,[3] shape,[4] aggregation,[5] and structure (solid *vs.* hollow),[6] as well as the dielectric properties of surrounding media.[7] For instance, the SPR peak of a thin film of gold is located at ~480 nm, while the SPR peak of an aqueous dispersion of 13 nm spherical gold colloids centers around 520 nm.[8] In a sense, silver or gold nanoparticles can be considered as inorganic chromophores with strong extinction. They have been actively explored for use as nanoscale devices for photon energy transport,[9] as medium for electron transport and charging,[10] as probes for scanning near-field optical microscopy,[11] and as active surfaces for surface-enhanced Raman[12] or fluorescence[13] scattering, and chemical or biological sensing.[14] Most of these applications require that the spectral position of SPR band can be conveniently tuned over a broad range.

Previous studies suggested that the SPR band of spherical silver or gold nanoparticles could only be slightly varied by changing their sizes in the range of 1 to 100 nm.[3,15] In contrast, the SPR band could be tuned in the spectral region from visible to near-infrared by working with nanoparticles of other morphologies or structures.[16] For example, El-Sayed and co-workers[16a] and Murphy and co-workers[16b] have shown that nanorods of gold exhibit two SPR peaks, with the wavelength of transverse mode located at 525 nm and the wavelength of longitudinal mode tunable in the spectral region from visible to near-infrared depending on their aspect ratios. Recent studies by Halas *et al.* suggest that the plasmon peak of gold nanoshells could be conveniently tuned to cover the spectral regime from 600 to 1200 nm by changing the diameter and wall thickness of the nanoshells.[16e] Here we describe a number of synthetic approaches to silver and gold nanoparticles with well-controlled compositions, morphologies, and structures. As shown in Fig. 1, these nanoparticles provide a platform to tune the SPR band in the spectral range from 400 to 750 nm.

Experimental

Chemicals and materials

Silver nitrate ($AgNO_3$, 99+%), chloroauric acid ($HAuCl_4$, 99.9%), and sodium borohydride ($NaBH_4$, 99%) were purchased from Aldrich (Milwaukee, WI) and used without any further purification. Anhydrous ethylene glycol (99.8%), and poly(vinyl pyrrolidone) (PVP, $M_w \approx 55000$) were also obtained from Aldrich. Sodium citrate was purchased from Fisher Scientific (Fair Lawn, NJ). Solid spherical colloids of gold and silver with various sizes were obtained as aqueous dispersions from Ted Pella (Redding, CA). Water purified with cartridges from Millipore (E-Pure, Dubuque, IA) to a resistivity of 18 MΩ.cm was used in the preparation of all samples.

Synthesis of gold/silver alloy nanoparticles

Gold/silver alloy nanoparticles were prepared following a procedure introduced by Turkevich *et al.*,[17] that involved the substitution of a precalculated number of moles of gold atoms by the equivalent number of moles of silver atoms. In this case, the total concentration of metal ions (including $HAuCl_4$ and $AgNO_3$) was kept as 0.25 mM. In the first step, an appropriate

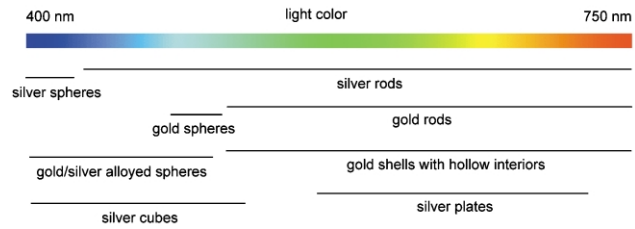

Fig. 1 A list of silver and gold nanoparticles having various morphologies, compositions, and structures, together with their typical locations of SPR bands in the visible regime.

 DOI: 10.1039/b212437h

volume of 30 mM $HAuCl_4$ aqueous solution was added to 50 mL water, and then heated to its boiling temperature. To this hot solution was added 20 mM aqueous $AgNO_3$ solutions of various volumes calculated accordingly. If $AgNO_3$ was mixed with $HAuCl_4$ at room temperature, the formation of solid silver chloride could lead to a failure for the synthesis. 2.5 mL of 1% sodium citrate solution was added to the refluxing solution and the solution was continued to reflux for another 30 min. The final solution was then left to cool to room temperature. Particles with gold molar fractions of 0 (*e.g.*, pure silver particles), 0.14, 0.25, 0.33, 0.50, 0.66, 0.75, 0.85, 0.91, and 1.00 were prepared through this process.

Synthesis of triangular nanoplates and circular nanodisks of silver

In a typical synthesis, 47.5 mL of purified water was deoxygenated by bubbling with nitrogen gas for 20 min before aqueous solutions of 30 mM sodium citrate (0.5 mL) and 5 mM silver nitrate (1 mL) were added. A 0.5 mL aliquot of freshly prepared sodium borohydride (50 mM) was quickly added to this mixture, followed by the addition of 0.5 mL aqueous solution of PVP (5 mg mL^{-1}). The mixture changed to a stable deep yellow color after the reaction had proceeded for another 30 min. Vigorous stirring was maintained during the entire process. The dispersion of silver nanoparticles was then transferred into 20 mL liquid scintillation glass vials (VWR) and irradiated for 40 h with a Halogen lamp (20 W, General Electric Co., Nela Park Cleveland, OH) equipped with a UV cutoff filter. The color of this dispersion became greenish blue, indicating the formation of triangular nanoplates of silver. The triangular nanoplates transformed into circular nanodisks after they were irradiated with a Model XX-15A UV lamp (λ = 356 nm, Spectroline, Spectronics Corporation, Westbury, NY) for another 8.5 h.

Synthesis of silver nanocubes

In the synthesis of silver nanocubes with edge length of 175 nm, 5 mL anhydrous ethylene glycol was heated at 160 °C for 1 h. 3 mL ethylene glycol solution of $AgNO_3$ (0.25 M) and 3 mL ethylene glycol solution of PVP (0.375 M in repeating unit) were simultaneously added to the hot ethylene glycol using a two-channel syringe pump (KDS-200, Stoelting Co., Wood Dale, IL) at a rate of 0.375 mL min^{-1}. The reaction was then continued with heating at 160 °C for another 45 min. The product was dominated by cubic nanoparticles, with a small amount (< 5%) of silver nanowires. These nanowires could be easily separated from nanocubes through filtration due to their large difference in dimension. In this case, the reaction mixture was diluted with water (25 times by volume) and filtered through Nucleopore membranes (Whatman, Clifton, NJ) that contained pores of 1 μm in diameter. The silver nanocubes could be recovered from ethylene glycol by centrifugation, and then redispersed into water. The silver nanocubes with smaller sizes could be synthesized by decreasing reaction time and/or the concentration of silver nitrate.

Synthesis of gold nanoshells

Gold nanoshells were prepared using the template-engaged replacement reaction between silver nanoparticles and an aqueous $HAuCl_4$ solution.[18] Silver nanoparticles with a mean diameter of 25 nm were synthesized using the polyol process.[19] In a typical procedure for the replacement reaction, a 250 μL aliquot of Ag nanoparticles was diluted with 5 mL water and then refluxed for 10 min. An 800 μL aliquot of 1 mM $HAuCl_4$ aqueous solution was added drop-wise to the refluxing dispersion. This mixture was then continuously refluxed until its color had become stable. The wall of these gold shells could be thickened using an electroless deposition process. In this case, 1 mL aqueous dispersion of gold nanoshells (silver had been completely consumed) was diluted with 4 mL water, and aliquots of 0.1 mM $HAuCl_4$ (0.5, 1.0, and 1.5 mL) were added drop-wise at room temperature. Finally, same volume of sodium citrate aqueous solution (0.4 mM) was added, continued with boiling for 20 min. Vigorous magnetic stirring was maintained throughout the entire synthesis.

Instrumentation

All UV-visible extinction spectra were recorded at room temperature using a Hewlett Packard 8452A spectrometer (Palo Alto, CA) with quartz cuvettes (1 cm optical path) as the containers. The samples for transmission electron microscopy (TEM) studies were prepared by placing small drops of reaction solutions on copper grids, and allowing the solvent to slowly evaporate at room temperature in a fume hood. The TEM images were taken using a JEOL microscope (1200EX II) operated at 80 kV. The scanning electron microscopy (SEM) images were obtained using a FEI field-emission microscope (Siron XL) operated at 5 kV.

Results and discussion

The ions of gold (*e.g.*, $HAuCl_4$) and silver (*e.g.*, $AgNO_3$) could be simultaneously reduced by sodium citrate in a refluxed aqueous solution to generate gold/silver alloy nanoparticles because of their close match in crystalline structure and lattice constants. The SPR of alloy nanoparticles was expected to exhibit only one peak, while two separated peaks for a mixture of gold and silver nanoparticles.[20] Fig. 2A shows the extinction spectra of particles of pure gold, pure silver and gold/silver alloy with various contents of gold. The SPR peaks of pure silver and gold particles were located at 405 and 516 nm, respectively. The SPR peaks of alloy particles fell between these two values and shifted to longer wavelengths as the content of gold was increased. The relationship between the peak position (λ_{max}) and the molar fraction of gold (x_{Au}) is plotted in Fig. 2B, and a linear dependence could be obtained by fitting with $\lambda_{max} = 412 + 1.13x_{Au}$. In this system, the SPR band of gold/silver alloy nanoparticles could be precisely tuned from 405 to 516 nm by simply changing the content of gold.

In addition to variation of chemical composition, control of morphology provides another means to tune the SPR band of metallic nanostructures as illustrated by the theoretical predictions.[2] However, the correlation between the geometrical shape of metal nanoparticles and their plasmon resonant spectral response has not been experimentally investigated due to the difficulties to obtain particles with well-defined shapes in bulk quantities. We have successfully prepared silver nanoparticles with various regular shapes, and earned a chance to systematically investigate the dependence of SPR response on morphology. For example, Fig. 3A shows the extinction spectra obtained from aqueous dispersions of silver nanoparticles having different morphologies, with their TEM images shown in Fig. 3B–D. The TEM image shown in Fig. 3B indicates that the silver nanoparticles characterized by a SPR peak at 391 nm were essentially spherical in shape, with a mean diameter of 5.6 ± 3.9 nm. The color of this dispersion turned from yellow to greenish blue after it had been irradiated with visible light for 40 h. TEM studies (Fig. 3C) revealed that the spherical colloids had been transformed into triangular nanoplates whose edge lengths varied from ~30 to ~90 nm. The corners of these nanoplates were rounded with various curvatures. This photo-induced

change in shape was also reflected in their extinction spectra (Fig. 3A). After irradiation, the solution exhibited three distinctive peaks located at 688, 485 and 334 nm. According to the theoretical calculation by Schatz *et al.*,[16f] these peaks could be assigned to the in-plane dipole, in-plane quadrupole, and out-of-plane quadrupole plasmon resonance bands, respectively. Circular nanodisks were also obtained after the dispersion of triangular nanoplates was irradiated with 365 nm UV light. This morphological transformation was accompanied with a color change from greenish blue to dark red. A TEM image of these nanodisks is shown in Fig. 3D, and their strongest SPR peak was blue-shifted to 585 nm (Fig. 3A). Note that the number of SPR peaks usually increases as the symmetry of nanoparticles is decreased: spherical nanoparticles (with C_s symmetry) exhibit only one peak, whereas two and three peaks are often observed for circular nanodisks (with $C_{\infty,h}$ symmetry) and triangular nanoplates (with D_{3h} symmetry), respectively.

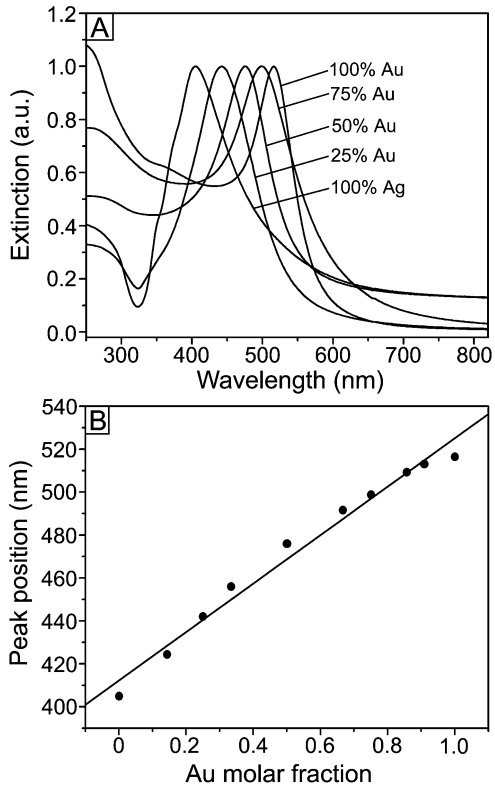

Fig. 2 (A) UV-visible extinction spectra of solid colloids made of pure silver, pure gold, and silver/gold alloys with various molar fractions of gold. All spectra were normalized against their peak extinctions. (B) A plot showing the linear dependence between the extinction peak position (λ_{max}) and the molar fraction (x_{Au}) of gold in the nanoparticles: $\lambda_{max} = 412 + 1.13x_{Au}$.

We have recently prepared a new class of silver nanoparticles with cubic shapes (or an O_h symmetry) through a modified polyol process.[21] Fig. 4A shows the SEM image of a typical sample of silver nanocubes, and indicate the large quantity and good uniformity that we were able to achieve using this approach. These silver nanocubes had a mean edge length of 175 nm. Smaller cubes could also be obtained by simply shortening the growth time and/or decreasing the concentration of silver precursor. For example, nanocubes with an average edge length of 80 nm were prepared under the same conditions as in Fig. 4A, except that the $AgNO_3$ concentration was reduced from 0.25 to 0.125 M and the growth time was shortened to 30 min. These nanocubes were found to exhibit unique SPR features as comparison with spherical nanoparticles. Fig. 4B shows the extinction spectra of cubic (the solid curve) and spherical (the dotted curve) silver nanoparticles that had roughly the same dimension (~ 80 nm). The isotropic, spherical nanoparticles displayed a strong SPR band around 430 nm, while the anisotropic, cubic nanoparticles exhibited three SPR bands (located at 350, 400, and 470 nm). As the size of silver nanocubes was increased from 80 to 175 nm, these three SPR peaks were red-shifted to 370, 438, and 560 nm (the dashed curve).

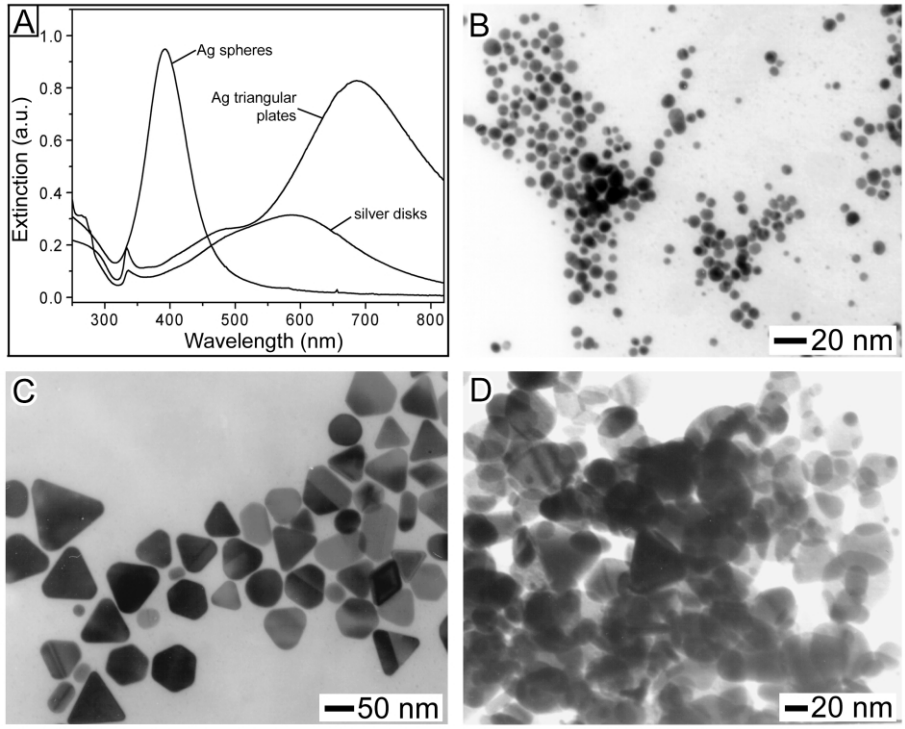

Fig. 3 (A) UV-visible extinction spectra of spherical nanoparticles, triangular nanoplates and circular nanodisks of silver that were stabilized with PVP and citrate. (B) A TEM image of the spherical silver nanoparticles. (C) A TEM image of the triangular nanoplates of silver that were formed by irradiating the sample in (B) with visible light for 40 h. (D) A TEM image of circular silver nanodisks that were prepared by irradiating the sample in (C) with 365 nm UV light for 8.5 h.

The SPR property of metallic nanoparticles could be further tuned by controlling their structure and local dielectric environment.[6,7] For example, gold nanoshells with hollow interiors have been synthesized *via* a template-engaged replacement reaction between silver nanoparticles with an aqueous $HAuCl_4$ solution.[18] A TEM image of such gold nanoshells is shown in Fig. 5A. The center portions of particles were lighter than their edges. Whereas the TEM image of gold solid colloids (Fig. 5B) shows that the central portions of them were darker than their edges. The curve e in Fig. 5C gives the extinction spectrum of an aqueous dispersion of silver nanoparticles (~25 nm in diameter) after they had been completely converted into gold nanoshells by reacting with $HAuCl_4$. Unlike gold solid nanoparticles, these gold nanoshells with hollow interiors had a SPR peak at 720 nm rather than 520 nm (the curve a, Fig. 5C), indicating that they had a high extinction coefficient in the red regime. Since the walls of these gold nanoshells were thinner than the mean free path (~50 nm) of free electrons in the bulk gold,[22] the contribution to dielectric function as caused by size-dependent electron scattering became sufficiently significant to be ignored. As a result, even a slight change in the shell thickness would greatly shift the wavelength of the SPR peak. These nanoshells with thin walls could be thickened by depositing additional gold onto their surfaces through an electroless process that involved the reduction of $HAuCl_4$ with sodium citrate. The curves b, c, and d in Fig. 5C show the extinction spectra of three samples of gold nanoshells after various amounts of $HAuCl_4$ and sodium citrate had been added. As more gold was plated onto the surfaces of these shells, their SPR peak continuously shifted to the blue side (from 720 to 560 nm). The color of these aqueous suspensions of gold nanoshells also changed from dark blue through purple to pink (as shown in Fig. 5D). Different from these gold nanoshells, the dispersion of gold solid nanoparticles with a mean diameter of ~30 nm had a red color and exhibited a sharp SPR peak centered at 520 nm.

To figure out the exact wall thickness for these nanoshells, we modified the Mie equation to calculate the scattering cross sections (and thus the extinction coefficients) of an individual gold nanoshell.[23] In a typical calculation, the nanoshell was assumed to have a spherical shape with a core diameter of 25 nm and whose interior was filled with the dispersion medium. The calculated wall thicknesses of gold nanoshells, whose SPR peak positions were same as curves b–e in Fig. 5C, were 6.0, 3.0, 2.0, and 1.65 nm, respectively. These calculated values were consistent with the results from TEM observations. The calculated spectra were also shown in Fig. 6A. It was worth noting that the SPR peak blue-shifted by 35 nm (from 720 to 685 nm) when the wall thickness increased from 1.65 to 2.0 nm (with a net increase of only 0.35 nm). This result further confirmed that the position of SPR band of gold nanoshells was extremely sensitive to their wall thickness. For gold nanoshell with a core diameter of 25 nm, their SPR peak position (λ_{max}) had a linear dependence on the reciprocal of wall thickness (t, unit in nm): $\lambda_{max} = 503 + 363/t$. This demonstration suggested that gold nanoshells with tunable SPR peaks could be synthesized by controlling the wall thickness.

When the surface plasmon mode is excited in gold, its intensity decays exponentially over a length scale of ~50 nm.[24] The modulation of SPR for surface-modified gold nanostructures should be dominated by the dielectric constant of the absorbate layers instead of the bulk solvent medium. As a result, gold nanostructures provide a means of detecting changes that occur in the region extremely close to the gold–solution interface. The sensitive response of SPR to environmental changes has been explored to optically detect binding events on the surfaces of colloidal particles. According to the Mie scattering theory,[2] any variation in the refractive index of the local environment around the colloid surface should lead to some changes in the intensity and/or position of the SPR peak. Such variations could arise from a compositional change in the

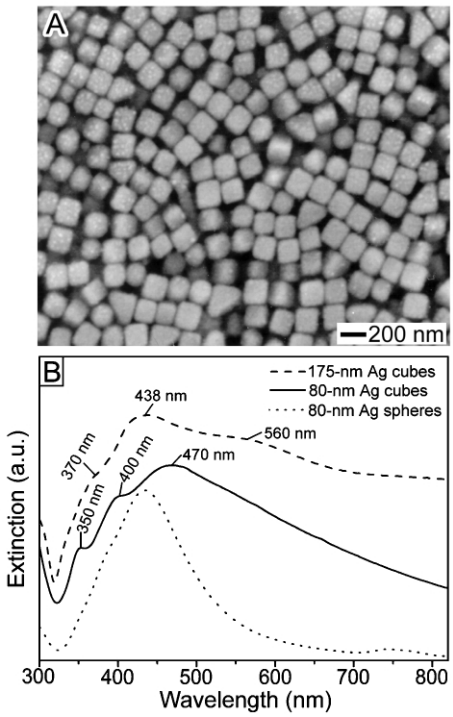

Fig. 4 (A) A typical SEM image of silver nanocubes with a mean edge length of 175 nm. (B) A comparison between the UV-visible extinction spectra of 80 nm spherical nanoparticles, 80 nm nanocubes, and 175 nm nanocubes of silver.

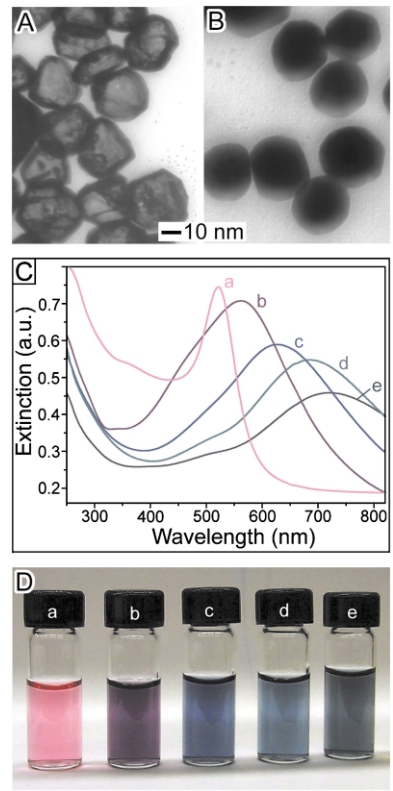

Fig. 5 TEM images of (A) gold nanoshells obtained by reacting 25 nm silver nanoparticles with $HAuCl_4$ and (B) gold solid colloids with diameter of ~30 nm. (C) UV-visible extinction spectra and (D) photographs of aqueous dispersions of gold nanoshells (e, ~25 nm in core diameter) after their surfaces had been electrolessly plated with gold of various thicknesses (b–d). As a comparison, the spectrum and photograph of a dispersion of gold solid colloids (~30 nm in diameter) were also shown (a).

dispersion medium, or from binding events that might occur at the colloid/solution interface. In general, an increase in the refractive index of surrounding medium often causes the SPR peak to shift to longer wavelengths. Based on this notion, a label-free colorimetric sensor has been demonstrated by Nath and Chilkoti to interrogate the biomolecular interactions in real time on the surfaces of gold colloids.[25] The sensitivity of such an optical probe also strongly depends on the size, shape, and dielectric properties of the metal colloids. Here, we compare the sensitivity of gold solid colloids and gold shells to the change of dispersion medium. The modified Mie equation was also used to calculate the scattering cross sections of a gold nanoshell and a gold solid colloid immersed in different solvents. In this case, the nanoshell and solid colloid were both assumed to have a spherical shape. Their extinction coefficients were calculated when the surrounding media were replaced with solvents having a range of different refractive indices. The interior of gold nanoshell was also assumed to be filled with the surrounding solvent. The calculated results illustrated that the extinction peak for both gold nanoshell (with a core diameter of 25 nm and wall thickness of 2 nm) and gold solid colloid (with diameter of 25 nm) were continuously red-shifted as the refractive index of surrounding medium increased, along with an increase in the extinction intensity. Fig. 7 plots the computed peak shift (relative to the sample with water as the dispersion solvent, n = 1.33) against the refractive index of the surrounding medium. The relative peak shift increased linearly with respect to the refractive index. The sensitivity factors ($\Delta\lambda_{max}/\Delta n$) were calculated as 66.5 and 328.5 nm per refractive index unit (RIU) for the solid colloid and nanoshell, respectively. These values implied that the gold nanoshells were ~5 times more sensitive to the environmental change when compared to gold solid colloids with roughly the same dimensions. Such an enhanced sensitivity to the environmental change might make gold nanoshells a useful platform to probe the binding events occurred on the surface.

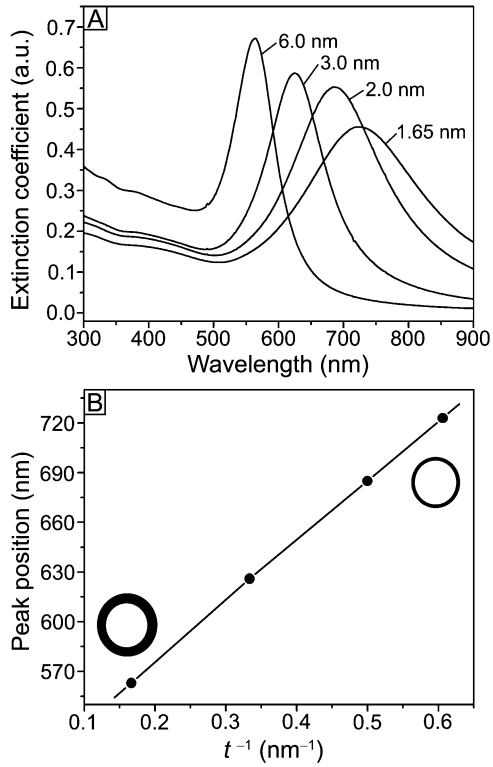

Fig. 6 (A) Extinction spectra calculated for spherical gold shells with a core diameter of 25 nm and various wall thickness: 1.65, 2.0, 3.0, and 6.0 nm. (B) The relationship between extinction peak position (λ_{max}) and the reciprocal of wall thickness (t^{-1}, nm^{-1}): λ_{max} = 503 + 363t^{-1}.

Conclusion

Spherical gold/silver alloy nanoparticles with various molar fractions of gold have been successfully synthesized by reducing their salt precursors with citrate. Their SPR band could be tuned in the range of 405–516 nm by simply changing the molar fraction of gold in the alloyed particles. Silver nanoparticles with various morphologies (such as spheres, triangular nanoplates, circular nanodisks, and nanocubes) have also been prepared in large quantities. Our spectral studies on these solid nanoparticles revealed that the number and position of SPR bands strongly depend on their symmetry: for example, the number of bands increased as the symmetry was decreased. Another class of nanostructures—gold nanoshells with hollow interiors—was also synthesized through a template-engaged replacement reaction by reacting silver nanoparticles with an aqueous $HAuCl_4$ solution. The wall thickness of nanoshells could be thickened using an electroless plating process that involved the reduction of $HAuCl_4$ with citrate salt. Spectroscopic investigation suggested that the SPR band of gold nanoshells could be tuned from ~520 nm up to near-infrared by changing the wall thickness. A comparative simulation study on the gold nanoshells and their solid counterparts suggested that the hollow nanostructures were more sensitive in detecting changes (both physical and chemical) that might occur on the surfaces.

In addition to the unique colors and highly sensitive response to environmental changes, these metallic nanoparticles could also serve as effective substrates for surface-enhanced Raman scattering (SERS). This enhancement effect is mainly due to the significant enhancement of electromagnetic field at the surface of metallic nanoparticle that is induced by the photo-excitation of conduction electrons. The local field on the metal surface increases to a maximum when the wavelength of incident light is consistent with the plasmon frequency of metallic nanoparticles.[26] The maximum enhancement factor also increases when the metallic nanoparticle has low symmetry and/or concentric structures (*e.g.*, metal shell with a dielectric core).[26,27] As a result, this technique should have high potentiality to probe single molecule when proper metallic particles presented in this work are used as the SERS-active substrates.

Acknowledgement

This work has been supported in part by an AFOSR-MURI grant awarded to the University of Washington, a Career Award from the NSF (DMR-9983893), a Fellowship from the David

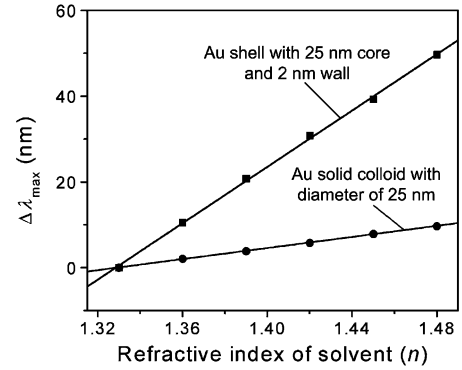

Fig. 7 Plots of the dependence of peak shift ($\Delta\lambda_{max}$, relative to the peak position calculated for water with n = 1.33) on the refractive index of surrounding medium. The sensitivity factors, $\Delta\lambda_{max}/n$, were 328.5 and 66.5 nm RIU^{-1} for gold nanoshell (with a core diameter of 25 nm and a wall thickness of 2 nm) and solid colloid (with diameter of 25 nm), respectively.

and Lucile Packard Foundation, a Research Fellowship from the Alfred P. Sloan Foundation, and a Camille Dreyfus Teacher Scholar Award.

References

1 (*a*) A. C. Templeton, W. P. Wuelfing and R. W. Murray, *Acc. Chem. Res.*, 2000, **33**, 27; (*b*) H. Bönnemann, J. Hormes and U. Kreibig, in *Handbook of Surface and Interfaces of Materials*, ed. H. S. Nalwa, Academic Press, San Diego, 2001, **vol. 3**, pp. 1–87; (*c*) M. A. El-Sayed, *Acc. Chem. Res.*, 2001, **34**, 257.

2 C. F. Bohren and D. R. Huffman, *Absorption and Scattering of Light by Small Particles*, Wiley, New York, 1983.

3 U. Kreibig and L. Genzel, *Surf. Sci.*, 1985, **156**, 678.

4 (*a*) D. Sarkar and N. J. Halas, *Phys. Rev. E*, 1997, **56**, 1102; (*b*) Y. Y. Yu, S. S. Chang, C. L. Lee and C. R. C. Wang, *J. Phys. Chem. B*, 1997, **101**, 6661.

5 J. P. Novak and D. L. Feldheim, *J. Am. Chem. Soc.*, 2000, **122**, 3979.

6 Y. Sun and Y. Xia, *Anal. Chem.*, 2002, **74**, 5297.

7 (*a*) C. L. Haynes and R. P. Van Duyne, *J. Phys. Chem. B*, 2001, **105**, 5599; (*b*) S. Underwood and P. Mulvaney, *Langmuir*, 1994, **10**, 3427.

8 F. X. Zhang, L. Han, L. B. Israel, J. G. Daras, M. M. Maye, N. K. Ly and C.-J. Zhong, *Analyst*, 2002, **127**, 462.

9 (*a*) T. W. Ebbesen, H. J. Lezec, H. F. Ghaemi, T. Thio and P. A. Wolff, *Nature*, 1998, **391**, 667; (*b*) J. B. Pendry, *Science*, 1999, **285**, 1687.

10 (*a*) K. D. Hermanson, S. O. Lumsdon, J. P. Williams, E. W. Kaler and O. D. Velev, *Science*, 2001, **294**, 1082; (*b*) S. Chen and Y. Yang, *J. Am. Chem. Soc.*, 2002, **124**, 5280.

11 (*a*) B. Knoll and F. Kellmann, *Nature*, 1999, **399**, 134; (*b*) E. J. Sánchez, L. Novotny and X. S. Xie, *Phys. Rev. Lett.*, 1999, **82**, 4014.

12 (*a*) T. Vo-Dinh, *Trends Anal. Chem.*, 1998, **17**, 557; (*b*) P. M. Tessier, O. D. Velev, A. T. Kalambur, J. F. Rabolt, A. M. Lenhoff and E. W. Kaler, *J. Am. Chem. Soc.*, 2000, **122**, 9554; (*c*) S. Nie and S. R. Emory, *Science*, 1997, **275**, 1102; (*d*) L. A. Dick, A. D. McFarland, C. L. Haynes and R. P. Van Duyne, *J. Phys. Chem. B*, 2002, **106**, 853.

13 (*a*) K. Sokolov, G. Chumanov and T. M. Cotton, *Anal. Chem.*, 1998, **70**, 3898; (*b*) P. Das and H. Metiu, *J. Phys. Chem.*, 1985, **89**, 4680.

14 (*a*) J. J. Storhoff, R. Elghanian, R. C. Mucic, C. A. Mirkin and R. L. Letsinger, *J. Am. Chem. Soc.*, 1998, **120**, 1959; (*b*) U. Kreibig, M. Gartz and A. Hilger, *Ber. Bunsen-Ges. Phys. Chem.*, 1997, **101**, 1593.

15 (*a*) A. Henglein and M. Giersig, *J. Phys. Chem. B*, 1999, **103**, 9533; (*b*) M. M. Alvarez, J. T. Khoury, T. G. Schaaff, M. N. Shafigullin, I. Vezmar and R. L. Whetten, *J. Phys. Chem. B*, 1997, **101**, 3706; (*c*) J. H. Hodak, A. Henglein and G. V. Hartland, *Pure Appl. Chem.*, 2000, **72**, 189.

16 (*a*) S. Link, M. B. Mohamed and M. A. El-Sayed, *J. Phys. Chem. B*, 1999, **103**, 3073; (*b*) N. R. Jana, L. Gearheart, S. O. Obare and C. J. Murphy, *Langmuir*, 2002, **18**, 922; (*c*) C. J. Murphy, *Science*, 2002, **298**, 2139; (*d*) C. J. Murphy and N. R. Jana, *Adv. Mater.*, 2002, **14**, 80; (*e*) S. J. Oldenburg, R. D. Averitt, S. L. Westcott and N. J. Halas, *Chem. Phys. Lett.*, 1998, **288**, 243; (*f*) R. C. Jin, Y. W. Cao, C. A. Mirkin, K. L. Kelly, G. C. Schatz and J. G. Zheng, *Science*, 2001, **294**, 1901.

17 J. Turkevich, P. C. Stevenson and J. Hillier, *Discuss. Faraday Soc.*, 1951, **11**, 55.

18 Y. Sun, B. T. Mayers and Y. Xia, *Nano Lett.*, 2002, **2**, 481.

19 P.-Y. Silvert, R. Herrera-Urbina and K. Tekaia-Elhsissen, *J. Mater. Chem.*, 1997, **7**, 293.

20 R. G. Freeman, M. B. Hommer, K. C. Grabar, M. A. Jackson and M. J. Natan, *J. Phys. Chem.*, 1996, **100**, 718.

21 Y. Sun and Y. Xia, *Science*, 2002, **298**, 2176.

22 D. Erts, H. Olin, L. Ryen, E. Olsson and A. Tholen, *Phys. Rev. B*, 2000, **61**, 12725.

23 (*a*) P. Mulvaney, *Langmuir*, 1996, **12**, 788; (*b*) A. C. Templeton, J. J. Pietron, R. W. Murray and P. Mulvaney, *J. Phys. Chem. B*, 2000, **104**, 564.

24 T. R. Jensen, L. Kelly, A. Lazarides and G. C. Schatz, *J. Clust. Sci.*, 1999, **10**, 295.

25 N. Nath and A. Chilkoti, *Anal. Chem.*, 2002, **74**, 504.

26 T. Vo-Dinh, *Trends Anal. Chem.*, 1998, **17**, 557.

27 J. P. Kottmann, O. J. F. Martin, D. R. Smith and S. Schultz, *Phys. Rev. B*, 2001, **64**, 235402.